Gene therapy for Duchenne muscular dystrophy

Naoki Suzuki, Yuko Miyagoe-Suzuki & Shin'ichi Takeda†

†Author for correspondence National Institute of Neuroscience, Department of Molecular Therapy, National Center of Neurology & Psychiatry, 4-1-1 Ogawa-higashi, Kodaira, Tokyo, 187-8502, Japan Tel.: +81 42 346 1720; Fax: +81 42 346 1750; takeda@ncnp.go.jp

Gene therapy has great potential to treat Duchenne muscular dystrophy. Among many proposed strategies to deliver a therapeutic gene to muscle, recombinant adeno-associated virus-mediated gene transfer is the most promising. The recent isolation of new adeno-associated virus serotypes from human and nonhuman primates provides the opportunity to develop vectors that can achieve the long-term expression of a therapeutic gene in muscles of the entire body without detrimental effects. To translate the results from small animal models to clinical trials in humans, further work using larger animal models, such as dystrophic dogs or nonhuman primates, is required. This review also discusses recent progress in other gene transfer-related therapeutic approaches, including targeted exon skipping and gene correction.

Keywords: adeno-associated virus vector, Duchenne muscular dystrophy, dystrophin, exon skipping, gene therapy

future medicine part of fsg

Duchenne muscular dystrophy (DMD), which affects one in 3300 males, is a devastating, progressive, muscle-wasting disease caused by mutations in the dystrophin gene [1,2]. Skeletal muscles in DMD are characterized by myofiber degeneration and progressive fibrous and fatty changes. There is, currently, no way to prevent muscle fiber necrosis and patients suffer severely from respiratory and cardiac complications in the second decade of life. The *DMD* gene is among the largest genes known, spanning 2.4 Mb at Xp21 and encoding a 427-kDa subsarcolemmal cytoskeletal protein, dystrophin, and several shorter isoforms (Dp260, Dp140, Dp116 and Dp71). The full-length dystrophin protein is composed of four domains: an N-terminal actin-binding domain, a central rod domain consisting of 24 spectrin-like repeats, a cysteine-rich domain and a C-terminal domain. Dystrophin binds actin at the N-terminal domain, β-dystroglycan at the cysteine-rich domain and dystrobrevin and syntrophins at the C-terminal domain, forming the dystrophin–glycoprotein complex (DGC) at the sarcolemma (Figure 1) [3]. A lack of dystrophin at the sarcolemma causes secondary loss of the DGC and other functional molecules, such as neuronal nitric oxide synthase (nNOS) [4] and aquaporin-4 [5]. Importantly, mutations in the genes encoding other members of the DGC cause several different types of muscular dystrophy. The mechanism of the degeneration and death of dystrophin-deficient myofibers is not yet fully understood, but it is believed that myofibers lacking dystrophin and the DGC at the cytoplasmic membrane are mechanically weak and highly susceptible to contraction-induced injury. As a result, the affected muscle experiences continuous cycles of myofiber death and regeneration, resulting in the gradual loss of myofibers and contractile force. In addition to mechanical weakness, abnormalities in calcium handling and changes in mitogen-activated protein (MAP) kinase and GTPase signaling in dystrophin-deficient muscle have been reported and proposed as underlying processes of muscular dystrophy [6,7].

At present, only corticosteroids are reported to effectively attenuate the progress of the disease [8], and current treatment options focus on respiratory and cardiac assistance and improvement of quality of life. Many research groups are still attempting to develop an effective therapy for DMD. In this review, we describe recent progress in gene and related therapies for DMD.

Recombinant adeno-associated virus vector: a promising tool for delivery of dystrophin gene to skeletal muscles

Among several gene transfer vectors and methods developed to date, the adeno-associated virus (AAV) vector is the most suitable to introduce the exogenous gene into postmitotic, nondividing myofibers. An AAV is a tiny, nonpathological, replication-defective virus, with a 4.7-kb single-stranded DNA genome, belonging to the parvovirus family. AAV vectors induce fewer immunological and inflammatory responses *in vivo* than adenovirus vectors [9]. Although the virus genome persists predominantly in episomal form, expression of the transferred gene lasts months to years in adult skeletal muscle. To date, more than 100 AAVs with distinct virus genome sequences have been isolated from humans, nonhuman primates and other species [10]. They display varying

10.2217/14796708.2.1.87 ISSN 1479-6708

degrees of similarity in their capsid proteins and show diverse tissue tropisms. More than nine AAV vectors have already been developed and evaluated in animal models as a tool for gene transfer *in vivo* (Table 1) [10]. Although the molecular mechanisms of tissue and cell tropisms of AAV vectors are not fully explained, they are likely to use different cellular receptors for entry into and binding to the host cells. The expression of the therapeutic genes is not permanent, mainly because recombinant (r)AAV does not replicate in the host and is barely incorporated into the genome of satellite cells. They are diluted out with the turnover of myofibers and, therefore, repeated administrations are required. New AAV serotypes would provide good options for follow-up treatments because they have the potential to evade pre-existing neutralizing antibodies against the previously used AAV serotype. However, to avoid the risks of *in vivo* vector delivery, it is important to better understand the vectors and the natural infection with the corresponding virus.

Generation of microdystrophin suitable for use in rAAV vectors

The rAAV vector is a promising tool for gene transfer to DMD muscle, but the limitation of the insertion size to 4.9 kb excludes incorporation of

Figure 1. Dystrophin forms the large dystrophin–glycoprotein complex at the sarcolemma, linking the basal lamina to the cytoskeletal actin.

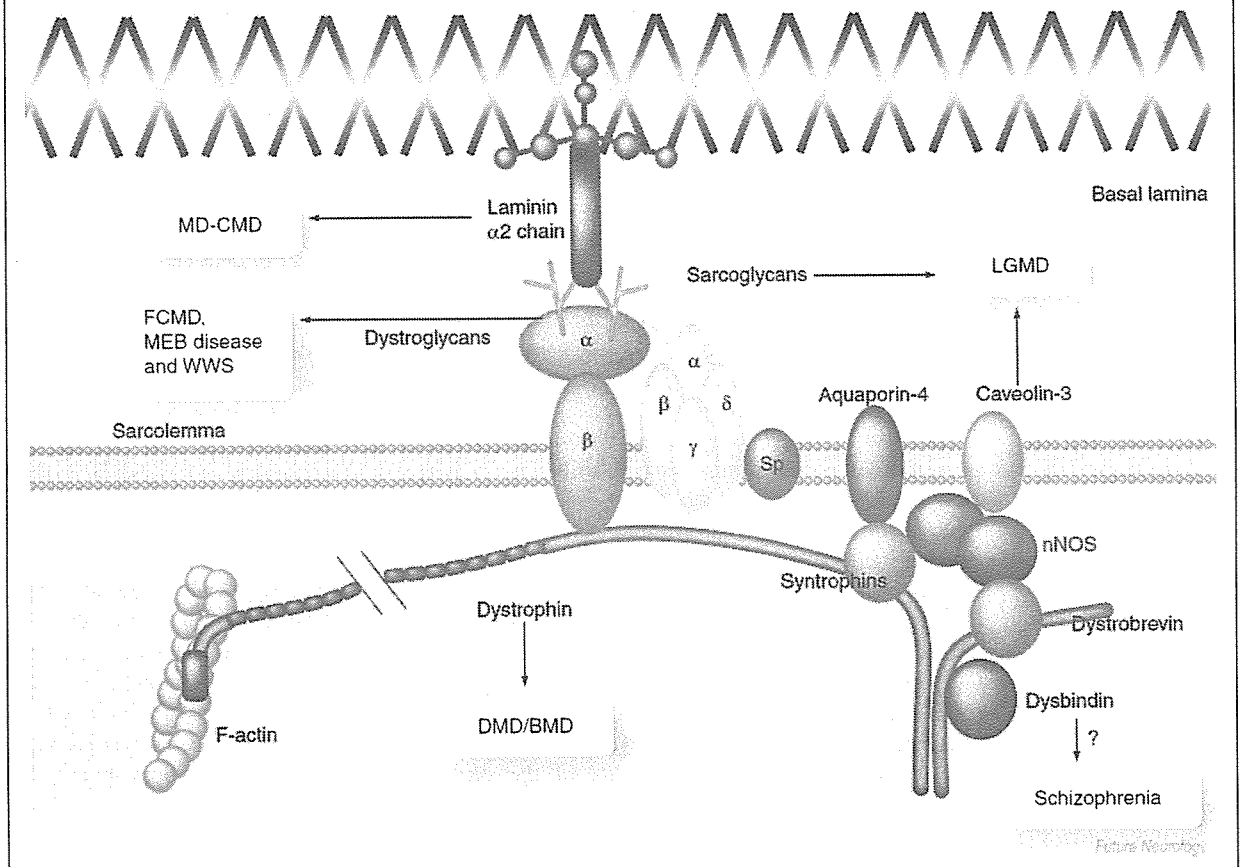

Mutations in the dystrophin gene end in the secondary loss of dystrophin–glycoprotein complex and other functional molecules, such as nNOS and aquaporin-4. Mutation in the laminin α2 chain gene causes congenital MD. Abnormal glycosylation of α-dystroglycan is commonly observed in FCMD, MEB disease and WWS. Abnormal glycosylation of α-dystroglycan also causes abnormalities in the eye and the CNS. Mutations in any of four sarcoglycan genes (α, β, γ and δ) result in LGMD. These observations emphasize the importance of dystrophin and associated molecules for muscle integrity. The dysbindin (*DTNBP1*) gene is one of the several putative susceptibility genes for schizophrenia.
BMD: Becker MD; DMD: Duchenne MD; FCMD: Fukuyama-type congenital MD; LGMD: Limb girdle MD; MD: Muscular dystrophy; MD-CMD: Merosin-deficient congenital MD; MEB: Muscle–eye–brain; nNOS: Neuronal nitric oxide synthase; WWS: Walker–Warburg syndrome.

Table 1. Characterization of nine serotypes of AAV vectors.

Serotype	Amino acid homology to AAV2 (%)	Isolated from	Tissue tropism				Delivery system
			Skeletal muscle	*Heart*	*Liver*	*CNS*	
1	84	NHP	+++	++	+	+	Local
2	100	Human	+	+	+	+	Local
3	88	Human		+	±	+	Local
4	64	NHP		+	±	+	Local
5	61	Human	+	+	++	++	Local
6	84	Human	++	++	+	+	Local, systemic
7	83	NHP	+++	+++	++	++	Local, systemic
8	84	NHP	+++	+++	+++	++	Local, systemic
9	83	Human	+++	+++	+++	++	Local, systemic

AAV: Adeno-associated virus; NHP: Nonhuman primate.
Reproduced from [65] © 2006, with permission from Sentan-Igaku Co.

a full-length dystrophin gene (14-kb mRNA, 11-kb open reading frame). To overcome this drawback, several groups have designed small dystrophins in which the long, central rod domains are largely deleted, and tested their functions in dystrophin-deficient *mdx* mice [11]. The functions of three types of microdystrophins (CS1, AX11 and M3; Figure 2) have been tested on microdystrophin-transgenic, dystrophin-deficient *mdx* mice, and it was observed that over-expressed CS1 with four repeats and three hinges almost completely ameliorated dystrophic phenotypes [12]. Therefore, a rAAV2 vector was constructed expressing CS1, driven by a skeletal muscle-specific muscle creatine kinase promoter [13], and was injected it into the anterior tibialis muscles of immunocompetent adult *mdx* mice. A total of 24 weeks after injection, 50% of myofibers, on average, expressed microdystrophin and the treated muscles demonstrated improved contractile force [14].

Systemic delivery of rAAV-serotype 6, 8 & 9 vectors

Systemic delivery systems for the treatment of DMD require improvement to enable transfer of the therapeutic genes to the complete musculature of the body, especially to the heart and diaphragm. Gregorevic and colleagues reported that intravenous injection of rAAV6 vectors efficiently delivered a microdystrophin gene to the

Figure 2. Structure of full-length dystrophin and constructs of mini- and microdystrophin (CS1, AX11 and M3).

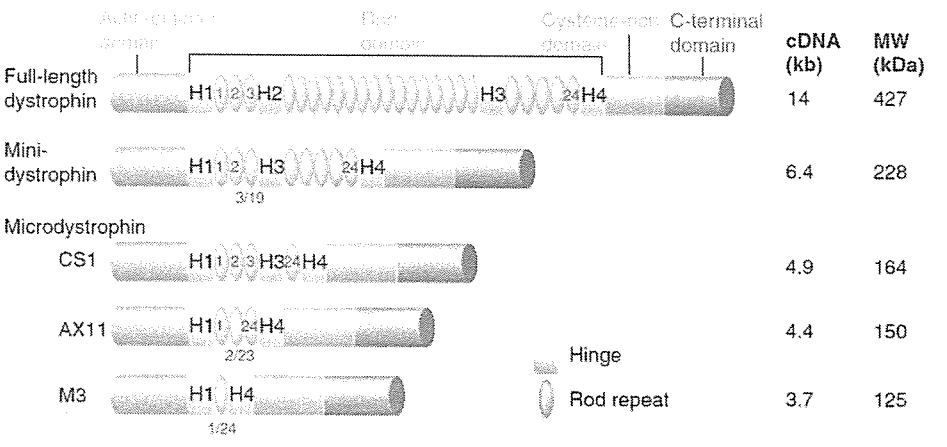

MW: Molecular weight.
Reproduced from [12] © 2002, with permission from Elsevier.

muscles of an adult mouse and the ratio of microdystrophin-positive fibers was increased when co-injected with vascular endothelial growth factor [15]. The widespread expression of microdystrophin was sufficient to correct susceptibility to contraction-induced injury and to lower serum creatine kinase levels [15]. Wang and colleagues, and Nakai and colleagues, demonstrated that AAV8 was more efficient than AAV6 or AAV1 at attaining systemic gene transfer, especially to the cardiac muscles of mice or hamsters, without pharmacological intervention [16,17]. More recently, Inagaki and colleagues reported that AAV9 vectors demonstrated robust systemic transduction in mice [18]. Remarkably, rAAV9 is superior to rAAV8 for gene delivery to cardiac muscle by systemic vector administration [18]. The molecular basis of the high transduction efficiency via the bloodstream is not fully understood, but these results are encouraging for researchers who are developing gene therapies for DMD patients. On the other hand, however, AAV8 or 9 vectors also increase transduction of nonmuscle tissues, such as liver (Table 1), which may be deleterious.

AAV vectors for human muscle

Animal models are indispensable for the evaluation of the efficacy and safety of AAV-mediated gene therapy of DMD, but a recent report on clinical gene transfer studies for hemophilia B demonstrated that the data obtained in preclinical studies in animals are not always predictive of vector efficacy in humans [19]. Certain human populations are exposed to AAVs in daily life: 50–96% are seropositive for AAV2 and at least a third have a neutralizing antibody to AAV2 [10]. Therefore, prior exposure to AAV2 explains the unsatisfactory results of clinical trials using rAAV2-factor IX gene transfer on hemophilia B patients [19]. The new serotypes of AAVs are reported to be prevalent in human and nonhuman primates. Prescreening of patients for neutralizing antibodies against the vector serotype and transient immune suppression would be required to avoid the elimination of rAAV particles by neutralizing antibodies.

Minidystrophin coded by two AAV vectors (dual vector system)

Microdystrophin proteins, with 3–4 spectrin-like repeats in the rod domain, do not completely compensate for the lack of full-length dystrophin. Among the constituents of DGC and its binding proteins, the expression of nNOS cannot be recovered through the introduction of microdystrophin. In an attempt to introduce a therapeutic gene larger than 4.7 kb into target cells, the trans-splicing approach, in which the gene is split between two rAAV vectors, each containing part of an intron with either a splice-acceptor or a splice-donor sequence, has been developed. After formation of head-to-tail concatamers, trans-splicing of the two RNA transcripts from the two different expression cassettes removes the intervening sequence, producing a functional mRNA larger than could be delivered in a single vector. This approach was employed to deliver a minidystrophin to *mdx* muscle [20], however, the coordinated nature of transcription and splicing makes this strategy highly inefficient *in vivo*.

Production of AAV vectors on a large scale

rAAV vector plasmids are generated by deleting the viral genome except for the inverted terminal repeats. To obtain recombinant AAV particles, double [21] or triple [22] transfection of the plasmids into human embryonic kidney (HEK)293 cells is performed to provide rep and capsid proteins and adenoviral helper functions (Figure 3). The obtained AAV vectors are further purified by CsCl gradient sedimentation or ion-exchange chromatography. In the case of rAAV2, it is estimated that at least 1×10^{13} vg/kg is required to treat humans with hemophilia, whereas the titer of the vectors prepared by this standard method is approximately $2–5 \times 10^{13}$ genome copies from 1×10^{9} HEK293 cells [13]. In clinical trials, an inexpensive, safe, large-scale system must be developed for the production of AAV. For example, Urabe and colleagues described a highly powerful production of rAAV using nonmammalian cell culture [23]. Okada and colleagues described a large-scale AAV vector production with active gassing [24].

Safety issues

Currently, most research on AAV-mediated gene transfer focuses on the systemic delivery of therapeutic genes via the blood circulation. Some have demonstrated the effectiveness of high-pressure arterial [25] or venous [26] infusion. These procedures seem to be powerful in transducing the therapeutic genes into targeted muscle groups, but the safety should be tested carefully in larger animal models. In particular, the mutagenic and carcinogenic potentials of recombinant genomes should be investigated, in addition to their potential for germline transfer after systemic delivery.

Figure 3. Production of pseudo-typed adeno-associated virus vectors in HEK293 cells.

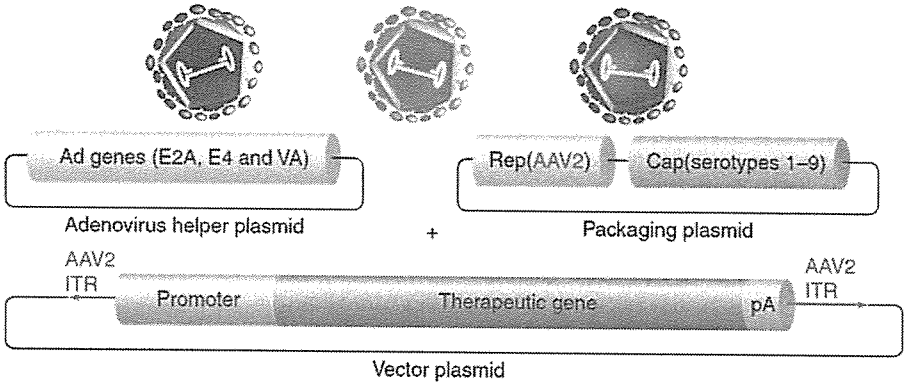

To obtain recombinant (r)AAV, three plasmids are transfected into human embryonic kidney (HEK)293 cells. The therapeutic gene is inserted between the two ITRs of the virus, with a ubiquitous or muscle-specific promoter. To avoid contamination of the helper adenovirus, plasmids encoding adenovirus-derived genes and *rep* and *cap* genes are cotransfected into the cells. Recently, the viral capsid gene from other AAV serotypes has been preferentially used in combination with the AAV2 vector to target the musculature body-wide *in vivo* after systemic delivery or to avoid pre-existing neutralization antibodies.
AAV: Adeno-associated virus; Cap: Capsid; ITR: Inverted terminal repeats.

Gutted adenoviral vectors expressing full-length dystrophin

Adenoviral vectors infect both dividing myoblasts and terminally differentiated muscle fibers, and possess a large insert capacity. However, early generations of adenoviral vectors, however, elicited substantial immune reactions in immunocompetent *mdx* mice and, hence, a rapid loss of transgene expression [27,28]. To circumvent this problem, a 'gutted' adenoviral vector, from which most viral DNA sequences are deleted, has been developed. Gutted adenoviral vectors are capable of carrying the large dystrophin gene together with regulatory sequences, and show reduced immunotoxicity compared with conventional adenoviral vectors [29–31]. Preparation of the gutted adenovirus vector requires a conventional adenovirus to supply replication and packaging functions *in trans*, and therefore has a high risk of helper virus contamination that may elicit immunological reactions upon delivery to tissues. In addition, recombinant adenoviral vectors remain comparatively toxic, especially in the liver, when administered systemically and have yet to achieve comparable transduction efficiency compared with AAV vectors.

Other vectors

A lentiviral vector is an alternative option for *in vivo* gene transfer into skeletal muscle. Kobinger and colleagues demonstrated that a lentiviral vector encoding minidystrophin targeted both satellite cells and myofibers of *mdx* mice and provided functional correction *in vivo* [32].

Direct injection of naked plasmid into dystrophic animals

Direct injection of a naked plasmid containing a full-length dystrophin cDNA into the muscles of DMD patients has been proposed as a promising treatment to restore the expression of dystrophin. The efficiency was low in animal models [33,34] and in a Phase I gene therapy clinical trial [35], but the dystrophin expression is relatively stable and evoked no signs of humoral or cellular immune responses. Experiments using mouse models demonstrated that the efficiency of gene transfer can be enhanced by electroporation coupled with the intramuscular application of hyaluronidase [36,37]. However, combination of electroporation and hyaluronidase administration would act to damage the muscle. The application to DMD patients is questionable. Hydrodynamic delivery of naked plasmid DNA expressing full-length dystrophin into the *mdx* mice has been reported to be effective [38]. Dystrophin expression was seen in 1–5% of the myofibers of the targeted muscle group of the hind limb for an extended period. To protect dystrophin-deficient muscles from muscle degeneration, repeated administration of plasmids would be required.

Ex vivo gene transfer into myogenic cells

Cell-mediated therapy can be used to deliver the normal dystrophin gene to dystrophic muscle. In particular, *ex vivo* transfer of a functional dystrophin gene into patients' satellite cells (myogenic progenitor cells usually located between myofibers and muscle basal lamina in a dormant state) and their progeny (myoblasts) is an attractive option for cell-based therapies for DMD since several methods to freshly purify satellite cells from muscle have been established [39,40]. A lentivirus vector would be the first choice for *ex vivo* mini- or microdystrophin gene transfer into autologous myogenic cells because it can infect freshly isolated satellite cells without lowering their proliferation and differentiation potential [Ikemoto *et al.*, Unpublished Data]. Stem cells other than satellite cells, such as muscle side population (SP) cells [41–43], mesoangioblasts [44], and AC133-positive human stem cells [43], have been reported to participate in muscle regeneration. Muscle SP cells are isolated by their ability to efflux Hoechst dye. Bachrach and colleagues demonstrated that SP cells from *mdx* (5cv) mice transduced with microdystrophin *ex vivo* were transplanted successfully via the tail vein and delivered human microdystrophin to the skeletal muscle of nonirradiated *mdx* (5cv) mice [45]. Recently, Dezawa and colleagues reported a novel method to induce muscle progenitor cells from human bone marrow stromal cells with a high efficiency [46].

Correction of endogenous genes

Gene conversion using chimeraplasts attempts to correct point mutations of the *DMD* gene in the cell. The first generation of chimeraplasts comprises hybrid RNA/DNA molecules that are homologous to a targeted gene, yet include one mismatched base. These hybrid nucleotides trigger gene conversion from a mutant to a functional allele via intranuclear DNA mismatch repair mechanisms. Injection of chimeric oligonucleotides into *mdx* mice resulted in the expression of full-length dystrophin in muscle fibers at the site of injection [47]. Gene correction mediated by chimeraplasts has also been demonstrated in the dystrophic golden retriever dog [48]. A second generation gene editing tool is a linear DNA oligonucleotide, 25-mer or longer containing a single central mismatch. This tool repaired single point mutations in the dystrophin gene with efficiencies comparable to that seen with chimeric RNA/DNA oligonucleotides, but yielded more consistent results [49]. Approximately 20% of DMD patients have single point mutations and, therefore, are potential targets of this therapeutic approach. However, gene repair techniques may not work for all mutations. Further data on the efficacy of the correction *in vivo* are required, using a range of point mutations of the dystophin gene.

Targeted exon skipping

Antisense oligonucleotides

DMD and *mdx* muscles have a few revertant fibers that express functional dystrophin [50,51]. This phenomenon is explained by aberrant splicing, which omits one or more exons and, as a result, restores a disrupted reading frame and dystrophin expression. Based on this observation, forced exon skipping is being developed as a future treatment to restore dystrophin expression from the mutated DMD gene in humans. The main tools for targeted exon skipping are antisense oligonucleotides (AOs). 2′-*O*-methyl-modified RNA on a phosphorothioate backbone, endowed oligonucleotides with greater resistance to nuclease degradation and, therefore, additional increases in stability were achieved [52–54]. Direct intramuscular injection of 2′-*O*-methyl phosphorothioate AOs resulted in a significant increase in the number of dystrophin-positive fibers (20%) in *mdx* mouse muscle [55]. Phosphoro-amide morpholino oligonucleotides have also proven to be effective in producing functional dystrophin in dystrophin-deficient muscle [56]. Weekly intravenous injections of morpholino AOs induced the expression of functional levels of dystrophin body-wide in skeletal muscles of the dystrophic *mdx* mouse and improved muscle function [57]. Based on the successful results in animal models, a clinical trial using AOs has already started in Leiden and is about to commence in the UK. Theoretically, AO-based exon skipping is applicable to 80% of dystrophin gene mutations. Furthermore, it is estimated that targeting just 12 exons restores the open reading frame of 75% of all deletions responsible for DMD.

AAV-mediated exon skipping

AOs display a limited half-life *in vivo*, and administration of AOs to patients must be repeated weekly or monthly. To obtain a longer-term effect, rAAV1 vectors expressing a modified U7 small nuclear RNA gene were used to direct exon skipping in *mdx* mice [58]. Following a single, high-pressure injection of the rAAV1/U7 vector

into the femoral artery of mdx mice, normal levels of dystrophin expression were restored and sustained for over 6 months. Although the initial study was limited to delivery to a single limb, this technique could be coupled with systemic delivery of AAV vectors of new serotypes.

Insulin-like growth factor-1 & myostatin blockade rescue dystrophin-deficient muscle

Myostatin (also known as growth and differentiation factor [GDF]8) is a transforming growth factor (TGF)-β family member that negatively regulates skeletal muscle growth, as evidenced by the increased musculature of the mice with a null mutation in this gene [59]. Mutation of the myostatin gene has also been found in human [60]. The myostatin-null child was reported to be muscular without any health problems at 4.5 years of age [60]. Myostatin blockade in *mdx* mice results in increases in both muscle mass and muscle strength and reductions in muscle fiber degeneration and serum creatine kinase levels [61]. Based on this observation, the recombinant human antibody against myostatin (MYO-029) is now being tested on adult muscular dystrophy patients.

Increased insulin-like growth factor (IGF)-1 within *mdx* myofibers reduces the breakdown of dystrophic muscle during the acute onset of muscle degeneration [62]. This mechanism of action can partly account for the long-term reduced severity of the dystrophic pathology in *mdx* mice overexpressing mIGF-1 and provides opportunities for therapeutic strategies [63].

Conclusion

Almost 20 years have passed since the discovery of dystrophin. Unfortunately, we have yet to find an effective therapy that can mitigate the dystrophic process. Numerous approaches are currently being explored, but many suffer from a variety of drawbacks. Among the gene therapy approaches to DMD under investigation, rAAV-mediated gene transfer is the most promising but still faces several obstacles. Other therapeutic approaches, including cell therapy and pharmacological intervention, would be used in complement with AAV-microdystrophin gene transfer.

Future perspective

An important step towards the clinical use of gene therapy is the evaluation of the efficacy and safety of gene transfer methods and protocols using animals larger than mice. We have established a beagle-based canine X-linked muscular dystrophy (CXMD) colony at the National Institute of Neuroscience in Japan ($CXMD_J$) and reported their severe phenotypes [64]. Beagle-based $CXMD_J$ is smaller and easier to handle than golden retriever CXMD, and is, therefore, a useful model for DMD. Preclinical studies using nonhuman primates would also be informative before clinical trials. Importantly, there are so many variables, even in a single treatment, such as myostatin blockade with antibodies, that more trials will be needed.

At present, gene therapy trials and related strategies face various hurdles and difficulties. Effective treatment of DMD may be achieved through a combination of different therapeutic approaches; for example, a combination of AAV vector-mediated gene transfer plus corticosteroid administration or myostatin blockage.

Acknowledgements

The authors are grateful to A Nishiyama and T Yokota for discussion and E Takahashi for help in preparing this manuscript. Studies in the authors' laboratory are supported by a Grant for Research on Nervous and Mental Disorders (16B-2), and Health Science Research Grants for Research on the Human Genome and Gene Therapy (H16-genome-003), for Research on Brain Science (H15-Brain-021, H18-Brain-019) from the Ministry of Health, Labor and Welfare, and Grants-in-Aid for Scientific Research (16590333, 18590392) from the Ministry of Education, Culture, Sports, Science and Technology.

Executive summary

Introduction

- Duchenne muscular dystrophy (DMD) is caused by mutations in the *DMD* gene, which encodes a 427-kDa subsarcolemmal cytoskeletal protein, dystrophin.
- At present, there is no treatment to arrest the progression of DMD and patients generally suffer from respiratory and/or cardiac complications in the second decade of life.
- Among several therapeutic strategies for this disease, recombinant adeno-associated virus (rAAV)-mediated gene transfer is the most promising.

Executive summary

Viral vector-mediated gene therapy

- AAV vectors drive long-term expression of the therapeutic gene in skeletal muscle *in vivo*, but the insertion size is limited to 4.9 kb.
- Functional, rod domain-deleted dystrophin (microdystrophin) can be incorporated into AAV vectors.
- New serotypes of AAV vectors have been isolated and developed as gene-transfer vectors, some of which transport the therapeutic genes to all the muscles of the body after systemic delivery.

Ex vivo *gene transfer into myogenic stem cells*

- Cell-mediated therapy can be used to deliver a normal dystrophin gene to dystrophic muscle in the hope that the delivered cells will participate in muscle-fiber regeneration in dystrophic muscle, express dystrophin and improve muscle function.
- Muscle satellite cells, side population cells, mesangioblasts, AC133-positive cells and bone marrow stromal cells are expected to be potential cell sources for cell-mediated therapy.

Gene correction & exon skipping using antisense oligonucleotides

- Chimeraplasts, which are chimeric RNA/DNA oligonucleotides homologous to a targeted gene (except for the inclusion of one mismatched base) can be used to direct the correction of a mutation by inducing preferential gene conversion from a mutant to a functional allele.
- Exon skipping using antisense oligonucleotides (AOs) targets transcribed RNA molecules to omit a nonsense mutation and restore a disrupted reading frame.
- Weekly intravenous injections of morpholino phosphorodiamidate (morpholino) AOs induce the expression of functional levels of dystrophin in skeletal muscles body-wide in the dystrophic *mdx* mouse.

Myostatin & insulin-like growth factor-1

- Blockage of myostatin and delivery of insulin-like growth factor-1 are effective to improve dystrophic phenotypes and the contractile force of dystrophin-deficient muscle.

Future perspective

- Preclinical studies using dystrophic dogs and nonhuman primates would be informative before human clinical trials.
- To overcome this devastating disease, multiple, diverse therapeutic strategies should be combined.

Bibliography

Papers of special note have been highlighted as either of interest (•) or of considerable interest (••) to readers.

1. Koenig M, Hoffman EP, Bertelson CJ, Monaco AP, Feener C, Kunkel LM: Complete cloning of the Duchenne muscular dystrophy (DMD) cDNA and preliminary genomic organization of the DMD gene in normal and affected individuals. *Cell* 50, 509–517 (1987).
2. Ray PN, Belfall B, Duff C *et al.*: Cloning of the breakpoint of an X;21 translocation associated with Duchenne muscular dystrophy. *Nature* 318, 672–675 (1985).
3. Engel AG, Ozawa E: Dystrophinopathies. In: *Myology (3rd Edition)*. Engel AG, Franzini-Armstrong C (Eds). McGraw-Hill. NY, USA, 961–1025 (2004).

• **Excellent text on muscular dystrophies.**

4. Brenman JE, Chao DS, Xia H, Aldape K, Bredt DS: Nitric oxide synthase complexed with dystrophin and absent from skeletal muscle sarcolemma in Duchenne muscular dystrophy *Cell* 82, 743–752 (1995).
5. Yokota T, Miyagoe Y, Hosaka Y *et al.*: Aquaporin-4 is absent at the sarcolemma and at perivascular astrocyte endofeet in α1-syntrophin knockout mice. *Proc. Japan Acad.* 76(Ser. B), 22–27 (2000).
6. Rando T: The dystrophin–glycoprotein complex, cellular signaling, and the regulation of cell survival in the muscular dystrophies. *Muscle Nerve* 24, 1575–1594 (2001).
7. Batchelor CL, Winder SJ: Sparks, signals and shock absorbers: how dystrophin loss causes muscular dystrophy. *Trends Cell. Biol.* 16, 198–205 (2006).
8. Biggar WD, Harris VA, Eliasoph L, Alman B: Long-term benefits of deflazacort treatment for boys with Duchenne muscular dystrophy in their second decade. *Neuromuscul. Disord.* 16, 249–255 (2006).

• **Long-term study that demonstrates that deflazacort has a very significant impact on the health and quality of life of boys with Duchenne muscular dystrophies (DMD), and is associated with few side effects.**

9. Blankinship MJ, Gregorevic P, Chamberlain JS: Gene therapy strategies for Duchenne muscular dystrophy utilizing recombinant adeno-associated virus vectors. *Mol. Ther.* 13, 241–249 (2006).

•• **Comprehensive review of recent progress in adeno-associated virus (AAV)-mediated gene therapy for DMD.**

10. Gao G, Vandenberghe LH, Wilson JM: New recombinant serotypes of AAV vectors. *Curr. Gene Ther.* 5, 285–297 (2005).

•• **Interesting review of the isolation strategy, evolution of new AAV serotypes, and their impact on gene therapy.**

11. Athanasopoulos T, Grahan IR, Foster H, Dickson G: Recombinant adeno-associated viral (rAAV) vectors as therapeutic tools for Duchenne muscular dystrophy (DMD). *Gene Ther.* 11, 109–121 (2004).

•• **Comprehensive review of recent progress in AAV-mediated gene therapy for DMD.**

12. Sakamoto M, Yuasa K, Yoshimura M *et al.*: Micro-dystrophin cDNA ameliorates dystrophic phenotypes when introduced into *mdx* mice as a transgene. *Biochem. Biophys. Res. Commun.* 293, 1265–1272 (2002).
13. Yuasa K, Sakamoto M, Miyagoe-Suzuki Y *et al.*: Adeno-associated virus vector-mediated gene transfer into dystrophin-deficient skeletal muscles evokes enhanced immune response against the transgene product. *Gene Ther.* 9, 1576–1588 (2002).
14. Yoshimura M, Sakamoto M, Ikemoto M *et al.*: AAV vector-mediated microdystrophin expression in a relatively small percentage of *mdx* myofibers improved the mdx phenotype. *Mol. Ther.* 10, 821–828 (2004).
15. Gregorevic P, Blankinship MJ, Allen JM *et al.*: Systemic delivery of genes to striated muscles using adeno-associated viral vectors. *Nat. Med.* 10, 828–834 (2004).

16. Wang Z, Zhu T, Qiao C *et al.*: Adeno-associated virus serotype 8 efficiently delivers genes to muscle and heart. *Nat. Biotechnol.* 23, 321–328 (2005).
- **Authors demonstrate that AAV8 vector is capable of introducing the therapeutic gene into the musculature of the whole body.**
17. Nakai H, Fuess S, Storm TA, Muramatsu S, Nara Y, Kay MA: Unrestricted hepatocyte transduction with adeno-associated virus serotype 8 vectors in mice. *J. Virol.* 79, 214–224 (2005).
18. Inagaki K, Fuess S, Storm TA *et al.*: Robust systemic transduction with AAV9 vectors in mice: efficient global cardiac gene transfer superior to that of AAV8. *Mol. Ther.* 14, 45–53 (2006).
19. Manno CS, Pierce GF, Arruda VR *et al.*: Successful transduction of liver in hemophilia by AAV-Factor IX and limitations imposed by the host immune response. *Nat. Med.* 12, 342–347 (2006).
20. Lai Y, Yue Y, Liu M *et al.*: Efficient *in vivo* gene expression by trans-splicing adeno-associated viral vectors. *Nat. Biotechnol.* 23, 1435–1439 (2005).
21. Grimm D, Kern A, Rittner K, Kleinschmidt JA: Novel tools for production and purification of recombinant adeno-associated virus vectors. *Hum. Gene Ther.* 18, 2745–2760 (1998).
22. Xiao X, Li J, Samulski RJ: Production of high-titer recombinant adeno-associated virus vectors in the absence of helper adenovirus. *J. Virol.* 72, 2224–2232 (1998).
- **One of the pioneering papers in adenovirus-free AAV preparation methods.**
23. Urabe M, Ding C, Kotin RM: Insect cells as a factory to produce adeno-associated virus type 2 vectors. *Hum. Gene Ther.* 13, 1935–1943 (2002).
24. Okada T, Nomoto T, Yoshioka T *et al.*: Large-scale production of recombinant viruses by use of a large culture vessel with active gassing. *Hum. Gene Ther.* 16, 1212–1218 (2005).
25. Gonin P, Arandel L, Van Wittenberghe L, Marais T, Perez N, Danos O: Femoral intra-arterial injection: a tool to deliver and assess recombinant AAV constructs in rodents whole hind limb. *J. Gene Med.* 7, 782–791 (2005).
26. Su LT, Gopal K, Wang Z *et al.*: Uniform scale-independent gene transfer to striated muscle after transvenular extravasation of vector. *Circulation* 112, 1780–1788 (2005).
27. Ishii A, Hagiwara Y, Saito Y *et al.*: Effective adenovirus-mediated gene expression in adult murine skeletal muscle. *Muscle Nerve* 22, 592–599 (1999).
28. Yamamoto K, Yuasa K, Miyagoe Y *et al.*: Immune response to adenovirus-delivered antigens upregulates utrophin and results in mitigation of muscle pathology in *mdx* mice. *Hum. Gene Ther.* 11, 669–680 (2000).
29. Dello Russo C, Scott JM, Hartigan-O'Connor D *et al.*: Functional correction of adult mdx mouse muscle using gutted adenoviral vectors expressing full-length dystrophin. *Proc. Natl Acad. Sci. USA* 99, 12979–12984 (2002).
30. Matecki S, Dudley RW, Divangahi M *et al.*: Therapeutic gene transfer to dystrophic diaphragm by an adenoviral vector deleted of all viral genes. *Am. J. Physiol. Lung Cell Mol. Physiol.* 287, L569–L576 (2004).
31. Dudley RW, Lu Y, Gilbert R *et al.*: Sustained improvement of muscle function one year after full-length dystrophin gene transfer into *mdx* mice by a gutted helper-dependent adenoviral vector. *Hum. Gene Ther.* 15, 145–156 (2004).
32. Kobinger GP, Louboutin JP, Barton ER, Sweeney HL, Wilson JM: Correction of the dystrophic phenotype by *in vivo* targeting of muscle progenitor cells. *Hum. Gene Ther.* 14, 1441–1449 (2003).
33. Braun S, Thioudellet C, Rodriguez P *et al.*: Immune rejection of human dystrophin following intramuscular injections of naked DNA in *mdx* mice. *Gene Ther.* 7, 1447–1457 (2000).
34. Liu F, Nishikawa M, Clemens PR, Huang L: Transfer of full-length *Dmd* to the diaphragm muscle of *Dmd* (*mdx/mdx*) mice through systemic administration of plasmid DNA. *Mol. Ther.* 4, 45–51 (2001).
35. Romero NB, Braun S, Benveniste O *et al.*: Phase I study of dystrophin plasmid-based gene therapy in Duchenne/Becker muscular dystrophy. *Hum. Gene Ther.* 15, 1065–1076 (2004).
36. Schertzer JD, Plant DR, Lynch GS: Optimizing plasmid-based gene transfer for investigating skeletal muscle structure and function. *Mol. Ther.* 13, 795–803 (2006).
37. Murakami T, Nishi T, Kimura E *et al.*: Full-length dystrophin cDNA transfer into skeletal muscle of adult *mdx* mice by electroporation. *Muscle Nerve* 272, 37–41 (2003).
38. Zhang G, Ludtke JJ, Thioudellet C *et al.*: Intraarterial delivery of naked plasmid DNA expressing full-length mouse dystrophin in the *mdx* mouse model of Duchenne muscular dystrophy. *Hum. Gene Ther.* 15, 770–782 (2004).
39. Montarras D, Morgan J, Collins C *et al.*: Direct isolation of satellite cells for skeletal muscle regeneration. *Science* 309(5743), 2064–2067 (2005).
40. Fukada S, Higuchi S, Segawa M *et al.*: Purification and cell-surface marker characterization of quiescent satellite cells from murine skeletal muscle by a novel monoclonal antibody. *Exp. Cell Res.* 296(2), 245–255 (2004).
41. Asakura A, Seale P, Girgis-Gabardo A, Rudnicki MA: Myogenic specification of side population cells in skeletal muscle. *J. Cell Biol.* 159, 123–134 (2002).
42. Uezumi A, Ojima K, Fukada S *et al.*: Functional heterogeneity of side population cells in skeletal muscle. *Biochem. Biophys. Res. Commun.* 341, 864–873 (2006).
43. Bachrach E, Li S, Perez AL *et al.*: Systemic delivery of human microdystrophin to regenerating mouse dystrophic muscle by muscle progenitor cells. *Proc. Natl Acad. Sci. USA* 101(10), 3581–3586 (2004).
44. Sampaolesi M, Torrente Y, Innocenzi A *et al.*: Cell therapy of α-sarcoglycan null dystrophic mice through intra-arterial delivery of mesoangioblasts. *Science* 301, 487–492 (2003).
45. Torrente Y, Belicchi M, Sampaolesi M *et al.*: Human circulating AC133$^+$ stem cells restore dystrophin expression and ameliorate function in dystrophic skeletal muscle. *J. Clin. Invest.* 114, 182–195 (2004).
46. Dezawa M, Ishikawa H, Itokazu Y *et al.*: Bone marrow stromal cells generate muscle cells and repair muscle degeneration. *Science* 309, 314–317 (2005).
47. Rando TA, Disatnik MH, Zhou LZ: Rescue of dystrophin expression in *mdx* mouse muscle by RNA/DNA oligonucleotides. *Proc. Natl Acad. Sci. USA* 97, 5363–5368 (2000).
48. Bartlett RJ, Stockinger S, Denis MM *et al.*: *In vivo* targeted repair of a point mutation in the canine dystrophin gene by a chimeric RNA/DNA oligonucleotide. *Nat. Biotechnol.* 18, 615–622 (2000).
49. Bertoni C, Morris GE, Rando TA: Strand bias in oligonucleotide-mediated dystrophin gene editing. *Hum. Mol. Genet.* 14, 221–233 (2005).

50. Hoffman EP, Morgan JE, Watkins SC, Partridge TA: Somatic reversion/suppression of the mouse *mdx* phenotype *in vivo*. *J. Neurol. Sci.* 99, 9–25 (1990).
51. Fanin M, Danieli GA, Cadaldini M *et al.*: Dystrophin-positive fibers in Duchenne dystrophy: origin and correlation to clinical course. *Muscle Nerve* 18, 1115–1120 (1995).
52. Wilton SD, Lloyd F, Carville K *et al.*: Specific removal of the nonsense mutation from the *mdx* dystrophin mRNA using antisense oligonucleotides. *Neuromuscul. Disord.* 9, 330–338 (1999).
53. Mann CJ, Honeyman K, Cheng AJ *et al.*: Antisense-induced exon skipping and synthesis of dystrophin in the *mdx* mouse. *Proc. Natl Acad. Sci. USA* 98, 42–47 (2001).
54. Mann CJ, Honeyman K, McClorey G, Fletcher S, Wilton SD: Improved antisense oligonucleotide induced exon skipping in the *mdx* mouse model of muscular dystrophy. *J. Gene Med.* 4, 644–654 (2002).
55. Lu QL, Mann CJ, Lou F *et al.*: Functional amounts of *dystrophin* produced by skipping the mutated exon in the *mdx* dystrophic mouse. *Nat. Med.* 9, 1009–1014 (2003).
56. Fletcher S, Honeyman K, Fall AM *et al.*: Dystrophin expression in the *mdx* mouse after localised and systemic administration of a morpholino antisense oligonucleotide. *J. Gene Med.* 8, 207–216 (2006).
57. Alter J, Lou F, Rabinowitz A *et al.*: Systemic delivery of morpholino oligonucleotide restores dystrophin expression bodywide and improves dystrophic pathology. *Nat. Med.* 12, 175–177 (2006).
•• **Demonstrates that weekly intravenous injections of morpholino antisense oligonucleotides induced expression of functional levels of dystrophin in skeletal muscles body-wide in the dystrophic *mdx* mouse, with resulting improvement in muscle function.**
58. Goyenvalle A, Vulin A, Fougerousse F *et al.*: Rescue of dystrophic muscle through U7 snRNA-mediated exon skipping. *Science* 306, 1796–1799 (2004).
•• **Describes persistent exon skipping of the mutated *DMD* gene in *mdx* muscle due to a single administration of an AAV vector expressing antisense sequences linked to a modified U7 small nuclear RNA.**
59. McPherron AC, Lawler AM, Lee SJ: Regulation of skeletal muscle mass in mice by a new TGF-β superfamily member. *Nature* 387, 83–90 (1997).
60. Schuelke M, Wagner KR, Stolz LE *et al.*: Myostatin mutation associated with gross muscle hypertrophy in a child. *N. Engl. J. Med.* 350, 2682–2688 (2004).
61. Bogdanovich S, Krag TO, Barton ER *et al.*: Functional improvement of dystrophic muscle by myostatin blockade. *Nature* 420, 418–421 (2002).
•• **Demonstrated that antimyostatin antibody treatment effectively improved the phenotypes of dystrophic *mdx* mice.**
62. Shavlakadze T, White J, Hoh JF, Rosenthal N, Grounds MD: Targeted expression of insulin-like growth factor-I reduces early myofiber necrosis in dystrophic *mdx* mice. *Mol. Ther.* 10, 829–843 (2004).
63. Barton ER, Morris L, Musaro A, Rosenthal N, Sweeney HL: Muscle-specific expression of insulin-like growth factor I counters muscle decline in *mdx* mice. *J. Cell Biol.* 157, 137–148 (2002).
64. Shimatsu Y, Yoshimura M, Yuasa K *et al.*: Major clinical and histopathological characteristics of canine X-linked muscular dystrophy in Japan, CXMD$_J$. *Acta Myol.* 24, 145–154 (2005).
• **Describes the phenotypes of a canine model of muscular dystrophy in the Beagle.**
65. Inagaki K, Nakai H: Recent progress in AAV vector (Japanese). *Cell Mol. Ther.* 6, 3–10 (2006).

Affiliations

- *Naoki Suzuki*
National Institute of Neuroscience, Department of Molecular Therapy, National Center of Neurology & Psychiatry, Kodaira, Tokyo 187-8502, Japan
Tel.: +81 42 346 1720;
Fax: +81 42 346 1750;
naoki@ncnp.go.jp
- *Yuko Miyagoe-Suzuki*
National Institute of Neuroscience, Department of Molecular Therapy, National Center of Neurology & Psychiatry, Kodaira, Tokyo 187-8502, Japan
Tel.: +81 42 346 1720;
Fax: +81 42 346 1750;
miyagoe@ncp.go.jp
- *Shin'ichi Takeda*
National Institute of Neuroscience, Department of Molecular Therapy, National Center of Neurology & Psychiatry, 4-1-1 Ogawa-higashi, Kodaira, Tokyo 187–8502, Japan
Tel.: +81 42 346 1720;
Fax: +81 42 346 1750;
takeda@ncnp.go.jp

BMC Cardiovascular Disorders

BioMed Central

Research article

Open Access

Cardiac involvement in Beagle-based canine X-linked muscular dystrophy in Japan (CXMD$_J$): electrocardiographic, echocardiographic, and morphologic studies

Naoko Yugeta[†1,2], Nobuyuki Urasawa[†2], Yoko Fujii[1], Madoka Yoshimura[2], Katsutoshi Yuasa[2], Michiko R Wada[2], Masao Nakura[3], Yoshiki Shimatsu[2], Masayuki Tomohiro[2], Akio Takahashi[4], Noboru Machida[5], Yoshito Wakao[1], Akinori Nakamura[2] and Shin'ichi Takeda*[2]

Address: [1]Department of Surgery I, School of Veterinary Medicine, Azabu University, Fuchinobe, Sagamihara, Kanagawa, 229-8501, Japan, [2]Department of Molecular Therapy, National Institute of Neuroscience, National Center of Neurology and Psychiatry, 4-1-1 Ogawa-higashi, Kodaira, Tokyo 187-8502, Japan, [3]Chugai Research Institute for Medical Science, Inc., 6598 Toyoda, Suwa, Nagano 392-0016, Japan, [4]Division of Laboratory Animal Resources, National Institute of Neuroscience, National Center of Neurology and Psychiatry, 4-1-1 Ogawa-higashi, Kodaira, Tokyo 187-8502, Japan and [5]Department of Veterinary Pathology, Faculty of Agriculture, Tokyo University of Agriculture and Technology, 3-5-8 Saiwai-cho, Fuchu, Tokyo 183-8509, Japan

Email: Naoko Yugeta - yugeta@b-star.jp; Nobuyuki Urasawa - urasawan@amber.plala.or.jp; Yoko Fujii - fujii@dc4.so-net.ne.jp; Madoka Yoshimura - yoshimur@ncnp.go.jp; Katsutoshi Yuasa - yuasa@ncnp.go.jp; Michiko R Wada - wadarin@ncnp.go.jp; Masao Nakura - nakuramso@chugai-pharm.co.jp; Yoshiki Shimatsu - shimatsu@ncnp.go.jp; Masayuki Tomohiro - tomhromy@banyu.co.jp; Akio Takahashi - akio_tk@ncnp.go.jp; Noboru Machida - machida@cc.tuat.ac.jp; Yoshito Wakao - wakao@azabu-u.ac.jp; Akinori Nakamura - anakamu@ncnp.go.jp; Shin'ichi Takeda* - takeda@ncnp.go.jp

* Corresponding author †Equal contributors

Published: 04 December 2006

BMC Cardiovascular Disorders 2006, 6:47 doi:10.1186/1471-2261-6-47

Received: 14 July 2006
Accepted: 04 December 2006

This article is available from: http://www.biomedcentral.com/1471-2261/6/47

Abstract

Background: Cardiac mortality in Duchenne muscular dystrophy (DMD) has recently become important, because risk of respiratory failure has been reduced due to widespread use of the respirator. The cardiac involvement is characterized by distinctive electrocardiographic abnormalities or dilated cardiomyopathy, but the pathogenesis has remained obscure. In research on DMD, Golden retriever-based muscular dystrophy (GRMD) has attracted much attention as an animal model because it resembles DMD, but GRMD is very difficult to maintain because of their severe phenotypes. We therefore established a line of dogs with Beagle-based canine X-linked muscular dystrophy in Japan (CXMD$_J$) and examined the cardiac involvement.

Methods: The cardiac phenotypes of eight CXMD$_J$ and four normal male dogs 2 to 21 months of age were evaluated using electrocardiography, echocardiography, and histopathological examinations.

Results: Increases in the heart rate and decreases in PQ interval compared to a normal littermate were detected in two littermate CXMD$_J$ dogs at 15 months of age or older. Distinct deep Q-waves and increase in Q/R ratios in leads II, III, and aVF were detected by 6–7 months of age in all CXMD$_J$ dogs. In the echocardiogram, one of eight of CXMD$_J$ dogs showed a hyperechoic lesion in the left ventricular posterior wall at 5 months of age, but the rest had not by 6–7 months of age. The left ventricular function in the echocardiogram indicated no abnormality in all CXMD$_J$ dogs by 6–7 months of age. Histopathology revealed myocardial fibrosis, especially in the left ventricular posterobasal wall, in three of eight CXMD$_J$ dogs by 21 months of age.

Conclusion: Cardiac involvement in $CXMD_J$ dogs is milder and has slower progression than that described in GRMD dogs. The distinct deep Q-waves have been ascribed to myocardial fibrosis in the posterobasal region of the left ventricle, but our data showed that they precede the lesion on echocardiogram and histopathology. These findings imply that studies of $CXMD_J$ may reveal not only another causative mechanism of the deep Q-waves but also more information on the pathogenesis in the dystrophin-deficient heart.

Background

Duchenne muscular dystrophy (DMD) is a common and lethal genetic disease characterized by progressive muscle wasting. It is an X-linked recessive disorder caused by mutations in the dystrophin gene, which encodes a cytoskeletal protein, dystrophin [1]. The absence of dystrophin is accompanied by a loss of dystrophin-glycoprotein complex at the sarcolemma and results in progressive degeneration of skeletal and cardiac muscle with fibrotic tissue replacement and fatty infiltration [2,3]. The onset of the disease occurs between 2 and 5 years of age, and most patients die of respiratory or cardiac failure [4,5]. Cardiac involvement, which occurs commonly in DMD patients, has increasingly become an important cause of death because recent clinical progress has reduced the risk of death due to respiratory failure [6,7].

Like dystrophin-deficient skeletal muscle, dystrophin-deficient cardiac muscle is replaced by fibrotic or fatty tissue, especially in the left ventricular posterobasal wall region [8-11]. Atrophic changes with loss of striation, vacuolation, fragmentation, or nuclear degeneration in the myocardium have also been reported [12]. Progressive involvement of the left ventricle leads to wall motion abnormality and results in dilated cardiomyopathy. In DMD patients, the electrocardiogram (ECG) may show tall R-waves in the right precordial leads, deep Q-waves in leads I, aVL, V5-6 or II, III, and aVF [8-13], as well as an increased heart rate, shortened PQ (PR) interval, conduction abnormalities or arrhythmias such as sinus arrhythmia, atrial ectopic beats, and ventricular premature complexes in DMD patients [13-16]. One of the electrocardiographic abnormalities, deep Q-waves, has been considered to be attributable to myocardial fibrosis [8,9,17]. Echocardiography indicates myocardial thickening, wall motion abnormalities, enlargement of the left ventricle, and left ventricular systolic and diastolic dysfunction. Hypokinesis of the posterobasal wall is consistent with the spreading fibrosis and significant decrease in the internal dimensions of the ventricles [14,15]. There are, however, many unresolved issues in cardiac involvement, such as the reason why the posterobasilar segment of the left ventricle is consistently the first lesion, whether extensive fibrosis involves the conduction system, the pathogenesis of inappropriate tachycardia or electrocardiographic abnormalities, and whether abnormal smooth muscle regulation affects the cardiomyopathy [18]. One way to clarify these problems is to study suitable animal models.

To date, the X-linked muscular dystrophy (*mdx*) mouse and the Golden retriever-based muscular dystrophy dog (GRMD) have been used for elucidation of the pathogenesis and development of therapy for DMD. The phenotypes of GRMD are more similar to DMD than that of the *mdx* mouse [19-21], and GRMD also shows similar electrocardiographic findings and progressive cardiomyopathy comparable to the cardiac involvement of DMD patients [20-23]. In this respect, GRMD is a useful model to explore cardiac involvement, but GRMD is very difficult to maintain because of their severe phenotypes. Mild phenotypes can be expected in small sized dogs such as Beagle, indicated by the cross-bred study by Valentine *et al.* [20]. Moreover, medium-sized Beagle is easy to handle or raise than GRMD, therefore they have definite advantages in animal housing or welfare. Therefore, we established a Beagle-based dog colony named canine X-linked muscular dystrophy in Japan ($CXMD_J$) [24]. In $CXMD_J$, involvement of the temporalis and limb muscles is observed from 2 months of age, and macroglossia, dysphagia, drooling, and joint contracture are apparent from 4 months of age; the phenotypes of $CXMD_J$ are thus almost comparable to GRMD [25]. In this study, we investigated the cardiac phenotypes in $CXMD_J$ using electrocardiography, echocardiography, and pathological examinations. Abnormalities on echocardiogram and cardiac pathology were detected from 12 months of age; however, the distinct deep Q-waves in leads II, III, and aVF on ECG were consistently observed by 6–7 months of age in all $CXMD_J$ dogs examined. The cardiac phenotypes of $CXMD_J$ were identical to but milder than those of GRMD described in the literature. Thus, $CXMD_J$ may also be a suitable animal model for elucidation of the above-mentioned problems.

Methods

Animals

We imported frozen GRMD semen and artificially inseminated a Beagle bitch. The carriers produced were mated with unrelated Beagles, and a Beagle-based canine X-linked muscular dystrophy ($CXMD_J$) breeding colony was established [24]. In this study, four normal male and eight affected male dogs of the third generation (G3) between 2 to 21 months of age were examined. All of the affected and normal dogs were descendents of a single affected

male, and were part of the $CXMD_J$ breeding colony at the General Animal Research Facility, National Institute of Neuroscience, National Center of Neurology and Psychiatry (NCNP) (Tokyo, Japan) or the Chugai Research Institute for Medical Science, Inc. (Nagano, Japan). The clinical and histopathological characteristics, except for cardiac involvement, of $CXMD_J$ dogs were recently described [25]. These dogs were cared for and treated in accordance with the guidelines provided by the Ethics Committee for the Treatment of Laboratory Middle-Sized Animals of the National Institute of Neuroscience, NCNP (Tokyo, Japan) or the Ethics Committee for Treatment of Laboratory Animal of Chugai Pharmaceutical Co., Ltd. (Tokyo, Japan). These studies were also approved by the Ethics Committee for the Treatment of Laboratory Middle-Sized Animals of NCNP (approved No. 13-03, 14-03, 15-03, 16-03, 17-03, and 18-03). All experiments were performed with consideration for preventing unnecessary pain.

Genotyping of $CXMD_J$ allele

Each affected or normal male dog was identified by genotyping. A snapback method of single-strand conformation polymorphism analysis was used to determine the GRMD allele as described previously [26].

Measurement of serum creatine kinase (CK)

Blood samples were obtained from the cephalic vein at sacrifice. Serum CK level was measured by colorimetric assay using a FDC3500 clinical biochemistry analyzer (FujiFilm Medical Co., Tokyo, Japan).

Electrocardiographic studies

Leads I, II, III, aVR, aVL and aVF were recorded in the right lateral recumbency using an ECG-922 electrocardiograph (Nihon Koden, Tokyo, Japan) [27]. All ECGs were obtained at a paper speed of 50 mm/sec and calibration of 10 mm/mV. First, the electrocardiography were performed in two $CXMD_J$ (III-302MA, III-303MA) and one normal littermate (III-301MN) dogs at 2, 3, 4, 6, 9, 12, 15, 18, and 21 months of age, and the heart rate (HR), intervals of PQ and QRS, and Q/R ratios were measured. However, in normal control and in $CXMD_J$, Q waves were not prominent in leads aVR and aVL, therefore, we measured the Q/R ratios in leads I, II, III and aVF. Next, we compared the HR, intervals of PQ and QRS, or Q/R ratios in I, II, III and aVF in eight $CXMD_J$ and four normal dogs at 6–7 months of age.

Echocardiographic studies

M-mode and two-dimensional echocardiography was performed using an EUB-8000 echocardiograph (Hitachi Medical Corporation, Tokyo, Japan). The thickness of the interventricular septum (IVS) and left ventricular posterior wall (LVPW) at end-diastole, left ventricular internal dimension at end-diastole (LVIDd) and systole (LVIDs), and fractional shortening (FS) were examined on normal and $CXMD_J$ dogs using M-mode echocardiography. We calculated the M-mode parameters based on multiple measurements of 5 consecutive heart cycles, or 3 or 5 representative heart cycles. We examined the parameters mentioned above and myocardial echogenicity in two $CXMD_J$ (III-302MA, III-303MA) and one normal littermate (III-301MN) dogs at 2, 3, 4, 6, 9, 12, 15, 18, and 21 months of age. We also examined the parameters mentioned above and myocardial echogenicity in six $CXMD_J$ (III-D53MA, III-D55MA, III-1803MA, III-D38MA, III-D02MA, III-D08MA) and three normal dogs (III-D56MN, III-1804MN, III-D03MN) at the time point just before euthanasia. Among those dogs, myocardial echogenicity in one $CXMD_J$ (III-D02MA) and its normal littermate (III-D03MN), and another $CXMD_J$ (III-D08MA) dogs were also examined at various time points.

Macroscopic and histopathological analyses

All dogs in this study underwent cardiac histological analysis. After a dog was given an overdose of intravenous pentobarbital, the whole heart was removed and immediately fixed in 15% buffered formalin. Formalin-fixed hearts were cross-sectioned, and samples were taken from the right and left ventricles at the apical papillary muscle and basal levels (each level containing the interventricular septum, anterior wall, lateral wall, and posterior wall). The tissue blocks were embedded in paraffin, and 10 μm sections were stained with hematoxylin and eosin or Masson's trichrome stain. Photographs were taken with a DAS Mikroskop LEITZ DMRB microscope (Leica, Wetzlar, Germany), using a digital still camera system HC-2500 (FujiFilm, Tokyo, Japan).

Statistics

Data are expressed as means +/- SE. Student's *t* test was used to evaluate differences between the two groups. A *p* value of less than 0.05 was considered to indicate statistical significance.

Results

Clinical profiles of $CXMD_J$

We recently reported the detailed clinical and histopathological characteristics of $CXMD_J$ except for cardiac phenotypes [25]. None of the dogs in the present study showed clinical signs of heart failure, and no murmur was present on auscultation in any $CXMD_J$ dog examined. We evaluated body and heart weight, the ratio of heart to body weight, and serum CK in eight $CXMD_J$ and four normal male dogs aged 6–21 months just before euthanasia (Table 1). There were no differences in body and heart weight and heart/body weight ratio between normal and $CXMD_J$ dogs. Serum CK levels in the $CXMD_J$ dogs ranged from 12,500 to 13 8,000 IU/1. These values were signifi-

cantly different from those in normal control dogs (60 to 515 IU/1). One 9-month-old $CXMD_J$ dog, III-D55MA, did not show any signs of respiratory or cardiac failure. When we tried to record a routine ECG of the dog, the dog struggled to escape from recording and then ceased moving. Immediately afterwards, we recorded ECG and the monitor showed an idioventricular rhythm. The dog died despite attempted cardiopulmonary resuscitation.

Electrocardiographic findings

The HR and PQ intervals of the affected littermates were no different from those recorded from a normal littermate at 12 months of age, but we detected an increase in HR and a decrease in PQ interval in the affected dogs after 15 months of age (Fig. 1A). The HR and PQ intervals were negatively correlated both in normal and affected dogs (data not shown). The QRS interval in the affected dogs did not differ from that in the normal littermate at any age (Fig. 1A). Prominent deep Q-waves were observed in limb leads II, III, and aVF in some $CXMD_J$ dogs, but not in the normal littermates, as shown in Fig. 1B. The Q/R ratios were definitely increased in the affected littermates at 6 months of age or older compared with the normal littermate (Fig. 1C). In all normal and $CXMD_J$ dogs at 6–7 months of age, the HR, and intervals of PQ and QRS were not different between the two groups of dogs (Fig. 2A), but the Q/R ratios in leads II, III, and aVF in the affected dogs were significantly higher than those in the normal dogs (Fig. 2B).

Echocardiographic findings

The thickness of LVIDd, IVS, and PW in two $CXMD_J$ (III-302MA, III-303MA) were not different from those in a normal littermate (III-301MN) by sequential analysis with advancing age (Fig. 3A). Those parameters were not different between other six $CXMD_J$ and three normal dogs, when examined just before euthanasia (Table 2). FS in III-302MA decreased with advancing age, and the value (27.3%) at 21 months of age was lower than that of the normal littermate, but was within normal range reported previously [28,29]. FS in the other seven $CXMD_J$ were normal, even just before euthanasia (Table 2). A mild hypokinesis of the left ventricular wall was detected in III-302MA at 21 months of age (Fig. 3B), but any clinical signs had not been developed in the dog.

The sequential studies of myocardial echogenicity with advancing age in III-302MA and in III-303MA demonstrated that the hyperechoic lesions in the left ventricular posterior wall were seen at 12 months of age or older (Fig. 4A, Table 3). In the subsequent examinations of six $CXMD_J$, we found the hyperechoic lesion in a $CXMD_J$, III-D08MA, at 5 months of age (Fig. 4B, Table 3), however the hyperechoic lesion was not detected in other four $CXMD_J$ at 5 to 7 months old (Fig. 4B, Table 3). One $CXMD_J$, III-D38MA, did not reveal any hyperechoic lesions when examined at 12 months of age, but has not been examined at 5 to 7 months of age (Table 3). Taken these echocardiographic data, it is considered that the cardiac functions in $CXMD_J$ were basically maintained well by 21 months of age, despite showing hyperechoic lesions of the left ventricle in limited numbers of $CXMD_J$.

Macroscopic and histopathological findings

The right and left ventricular walls were examined macroscopically and histopathologically in four normal and eight affected male dogs at the ages shown in Table 1. The base view of the formalin-fixed heart did not show any macroscopic lesions in III-1803MA at 7 months and III-302MA at 21 months of age (Fig. 5A) like other affected dogs (data not shown). No histopathological abnormality was found in the posterior wall of the left ventricle of

Table 1: Clinical profiles of normal and $CXMD_J$ male dogs

	Age (mo)	BW(g)	HW(g)	HW/BW (%)	Serum CK (IU/l)
Normal dogs					
III-D56MN	6	12.0	95.1	0.97	515
III-1804MN	7	13.6	110.0	0.81	215
III-D03MN	14	13.1	127.0	0.84	215
III -301 MN	21	14.4	120.0	0.96	60
$CXMD_J$ dogs					
III-D53MA	6	9.6	91.9	0.90	63,100
III-D55MA	7	10.0	80.0	0.80	42,000
III-1803MA	9	14.4	128.6	0.69	69,100
III-D38MA	12	11.4	78.8	1.01	138,000
III-D02MA	15	9.1	92.0	0.87	17,600
III-D08MA	15	12.0	104.3	0.97	40,700
III-302MA	21	12.4	120.0	0.86	12,500
III-303MA	21	13.9	120.0	0.80	23,000

BW, body weight; HW, heart weight; HW/BW, heart weight/body weight ratio; * $p < 0.01$ normal dogs *vs* $CXMD_J$ dogs

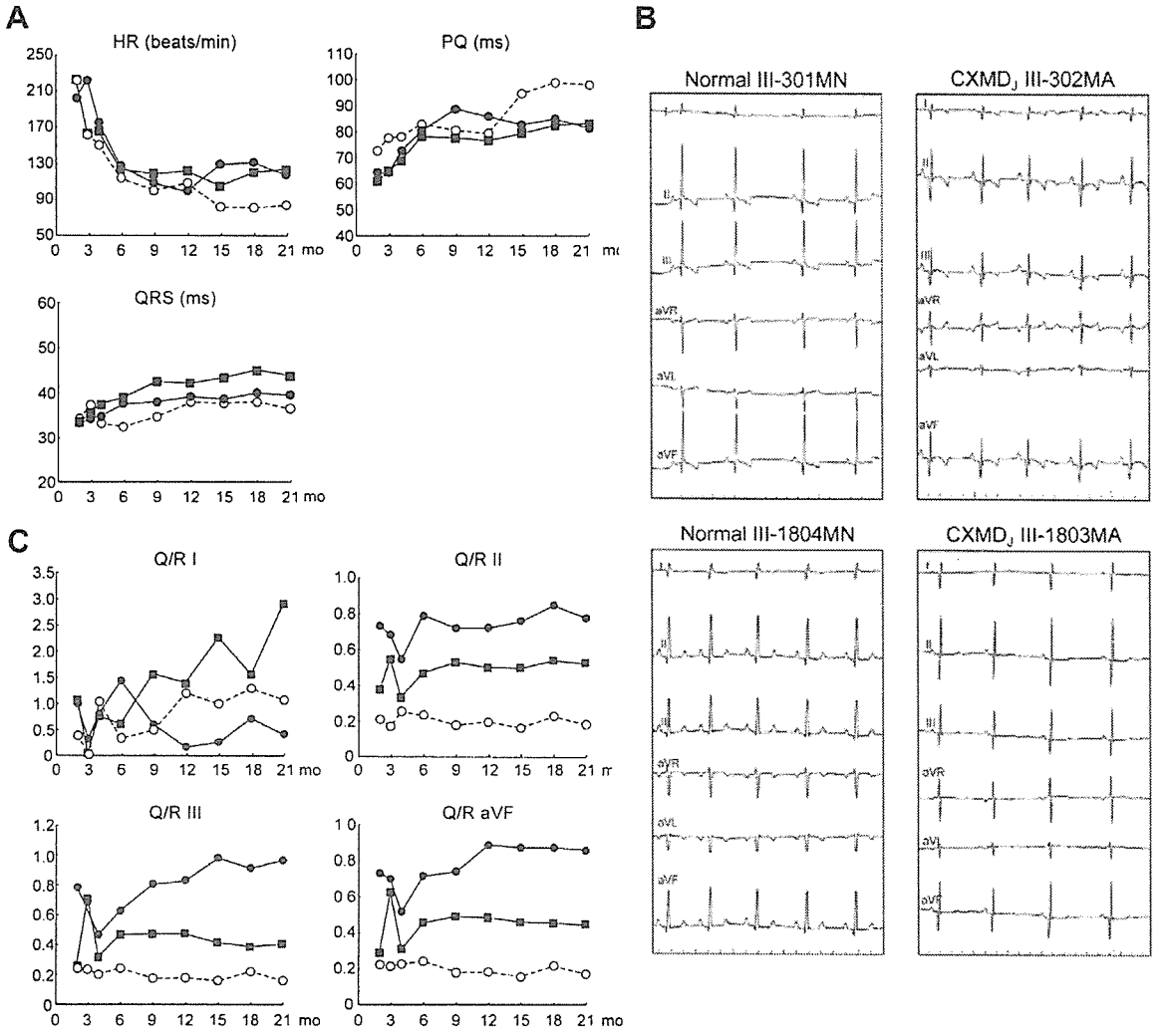

Figure 1

Electrocardiographic findings in CXMD$_J$ A: Sequential studies in electrocardiographic parameters with advancing age in normal and CXMD$_J$ dogs. Heart rate (HR) (beats/min), PQ interval (ms), and duration (ms) of QRS complex on ECG in a normal littermate III-301MN (open circle), and CXMD$_J$ dogs III-302MA (closed circle) and III-303MA (closed square) at 2, 3, 4, 6, 9, 12, 15, 18, and 21 months of age. **B**: Representative ECGs in normal and CXMD$_J$ male dogs. ECGs were recorded from normal dogs, III-301MN and III-1804MN, and CXMD$_J$ dogs, III-302MA and III-1803MA, at 6 months of age. Distinct deep Q waves were present in the CXMD$_J$ dogs. Leads were recorded at 50 mm/s, 1 cm/mV. **C**: Sequential studies in Q/R ratios with advancing age in limb leads I, II, III, and aVF in normal and CXMD$_J$ dogs. Q/R ratios in limb leads I, II, III, and aVF in a normal littermate III-301MN (open circle), and the CXMD$_J$ dogs III-302MA (closed circle) and III-303MA (closed square) at 2, 3, 4, 6, 9, 12, 15, 18, and 21 months of age.

affected dogs III-1803MA, III-D55MA, and III-D02MA (Fig. 5B), and other affected dogs under the age of 12 months (III-D53MA, III-D38MA). On the other hand, moderate fibrosis in the left ventricular wall, especially on the posterior side, was detected in an affected dog, III-302MA, at 21 months (Fig. 5B) as well as in III-D08MA at

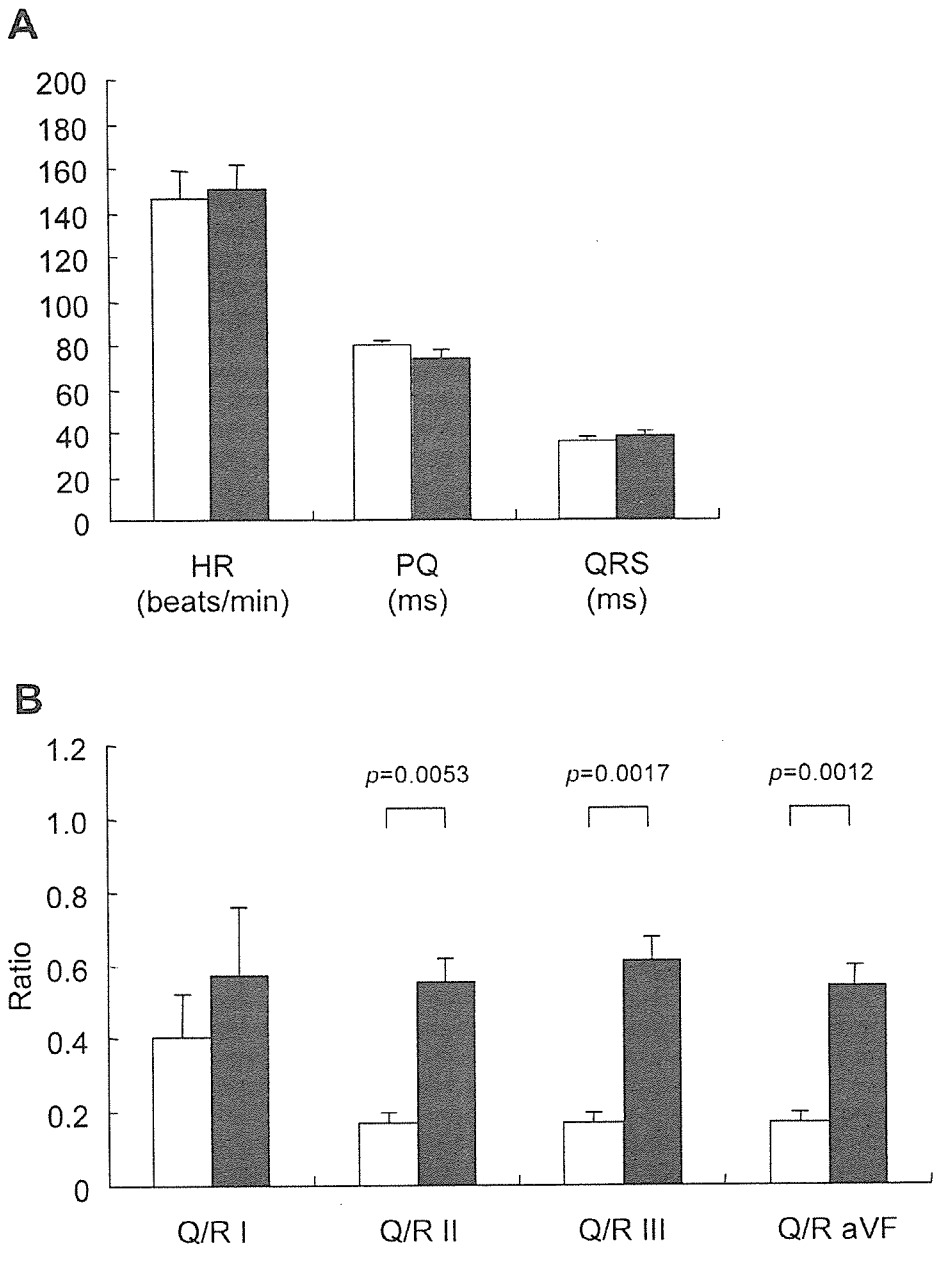

Figure 2
Comparison of electrocardiographic parameters and Q/R ratios between normal and $CXMD_J$ dogs at 6–7 months of age A. Heart rate (HR) (beats/min), PQ interval (ms), and duration of QRS complex (ms) on ECG in normal (n = 4) and $CXMD_J$ (n = 8) dogs at 6–7 months of age. White columns indicate normal dogs, and black columns represent $CXMD_J$ dogs. Bar shows mean +/- SE. **B.** Q/R ratios in limb leads I (Q/R I), II (Q/R II), III (Q/R III), and aVF (Q/R aVF) on ECG in normal (n = 4) and $CXMD_J$ (n = 8) dogs at 6–7 months of age. White columns indicate normal dogs, and black columns represent $CXMD_J$ dogs. Bar shows mean +/- SE.

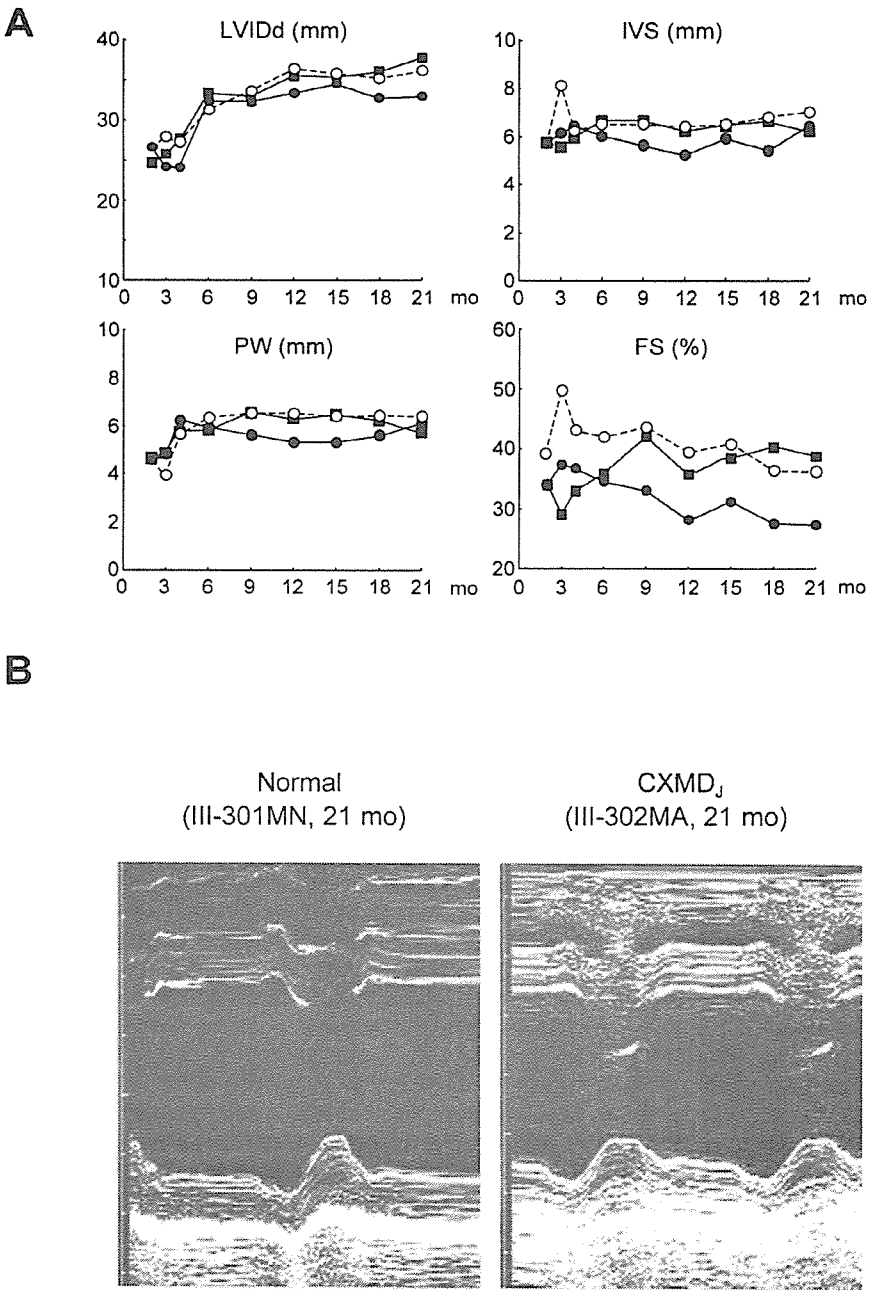

Figure 3
Cardiac function by echocardiography in CXMD$_J$ A: Sequential studies in echocardiographic parameters with advancing age in normal and CXMD$_J$ dogs. LVIDd (mm), IVS and PW thickness (mm), and FS (%) in a normal littermate III-301MN (open circle), and the CXMD$_J$ dogs III-302MA (closed circle) and III-303MA (closed square) at 2, 3, 4, 6, 9, 12, 15, 18, and 21 months of age. **B**: M-mode echocardiogram in a normal littermate III-301MN, compared to the CXMD$_J$ dog III-302MA at 21 months of age. Hypokinesis of the left ventricular posterior wall was observed in the CXMD$_J$ dog.

Table 2: Echocardiographic findings in normal and $CXMD_J$ male dogs

	Age (mo)	LVIDd (mm)	LVIDs (mm)	IVS (mm)	PW (mm)	FS (%)
Normal male dogs						
III-D56MN	6	34.2	12.5	6.6	5.6	63.5
III-1804MN	7	30.7	18.9	8.2	7.4	38.4
III-D03MN	14	32.8	16.8	10.0	9.4	48.7
III-301 MN	21	36.1	23.0	7.0	6.4	36.2
$CXMD_J$ male dogs						
III-D53MA	6	29.7	19.7	8.0	7.2	33.8
III-D55MA	7	28.7	15.4	6.3	6.3	46.5
III-1803MA	7	32.5	16.7	5.8	7.5	48.5
III-D38MA	12	30.3	18.8	8.4	5.8	37.8
III-D02MA	15	27.5	17.3	9.1	8.8	37.0
III-D08MA	15	39.5	24.9	5.9	5.9	36.9
III-302MA	21	32.9	23.9	6.4	6.1	27.3
III-303MA	21	37.6	23.1	6.2	5.7	38.6

Age, age at examination; LVIDd, LV internal dimension diastolic; LVIDs, LV internal dimension systolic; IVS, intraventricular septum thickness; PW, posterior wall thickness; FS, fractional shortening

15 months and III-303MA at 21 months of age (data not shown). We found that the right ventricular walls were kept intact in all $CXMD_J$ dogs examined.

Discussion

In electrocardiographic findings, an increased HR and a shortened PQ interval have been reported in both DMD patients [13] and GRMD [22]. These findings were also observed in $CXMD_J$ dogs. Increased sympathetic activity and decreased parasympathetic activity have been observed in DMD patients and are associated with disease progression [30]; therefore, autonomic dysfunction in dystrophin deficiency might affect these parameters. It has been reported that HR is negatively correlated with PQ interval in normal Beagle dogs and it may be ascribed to a parasympathetic input at the level of the AV node [31]. The negative correlation between HR and PQ intervals was also found in affected dogs, indicating the parasympathetic input was maintained well even in affected dogs at AV node level. The QRS duration was within normal limits in the $CXMD_J$ dogs, which is compatible with most cases of DMD [13]. Another peculiar electrocardiographic finding in DMD is the deep and narrow Q-waves in I, aVL and V6 or in II, III and aVF [10,13,16,32]. $CXMD_J$ dogs also showed prominent Q-waves and increases in the Q/R ratio in leads II, III, and aVF, findings that are consistent with those in GRMD [23]. In all $CXMD_J$ dogs examined, the distinct deep Q-waves were recognized by 6–7 months of age, which is earlier than the other abnormal electrocardiographic parameters, and the Q/R ratio in affected dogs remained high from 6 to 21 months of age. Actually, the prominent Q-wave and increase in Q/R ratio were also detected in some of the $CXMD_J$ dogs at around 2 months of age (Fig. 1C), but it is difficult to evaluate the degree of the Q/R ratio increase before 3 months of age because the QRS vector is almost exclusively directed to the right and varies significantly in the weeks after birth [33]. A previous report described GRMD dogs ranging from 6 months to > 2 years as having deep Q-waves and increased Q/R ratios in leads II, III, and aVF [23]. The Q-waves, however, might have been seen earlier and regarded as normal variants or not have been considered important for the reasons mentioned above.

Hyperechoic lesions indicating myocardial fibrosis in the posterobasal left ventricular wall have been detected by echocardiography in GRMD dogs as well as DMD patients [22,23]. Moise *et al.* reported that hyperechoic lesions were first detected in eight of eleven GRMD dogs (73%) by 6–7 months of age and that they correlated with histologically recognizable areas of mineralization and corresponded to the progression of fibrosis [23]. In our study, one of eight of $CXMD_J$ dogs showed a hyperechoic lesion in the left ventricular posterior wall, but the rest had not by the age of 6–7 months (Table 3, Fig. 4). The hyperechoic lesion in the left ventricular posterior walls was detected in both III-302MA and III-303MA, but not early as 12 months of age (Table 3). The results of echocardiography indicated that the cardiac involvement in $CXMD_J$ is milder than that in GRMD. Echocardiography did not reveal particular left ventricular dysfunction in any $CXMD_J$ dog by 21 months of age, but a mild hypokinesis of the left ventricular wall was observed in III-302MA at 21 months of age (Fig. 3B). The dysfunction found in the dog, however, was mild and the dog had no cardiac symptom. Moise *et al.* reported that three of the six GRMD dogs > 2 years of age showed a decrease in fractional shortening, but did not mention at what age the abnormal cardiac findings appeared.

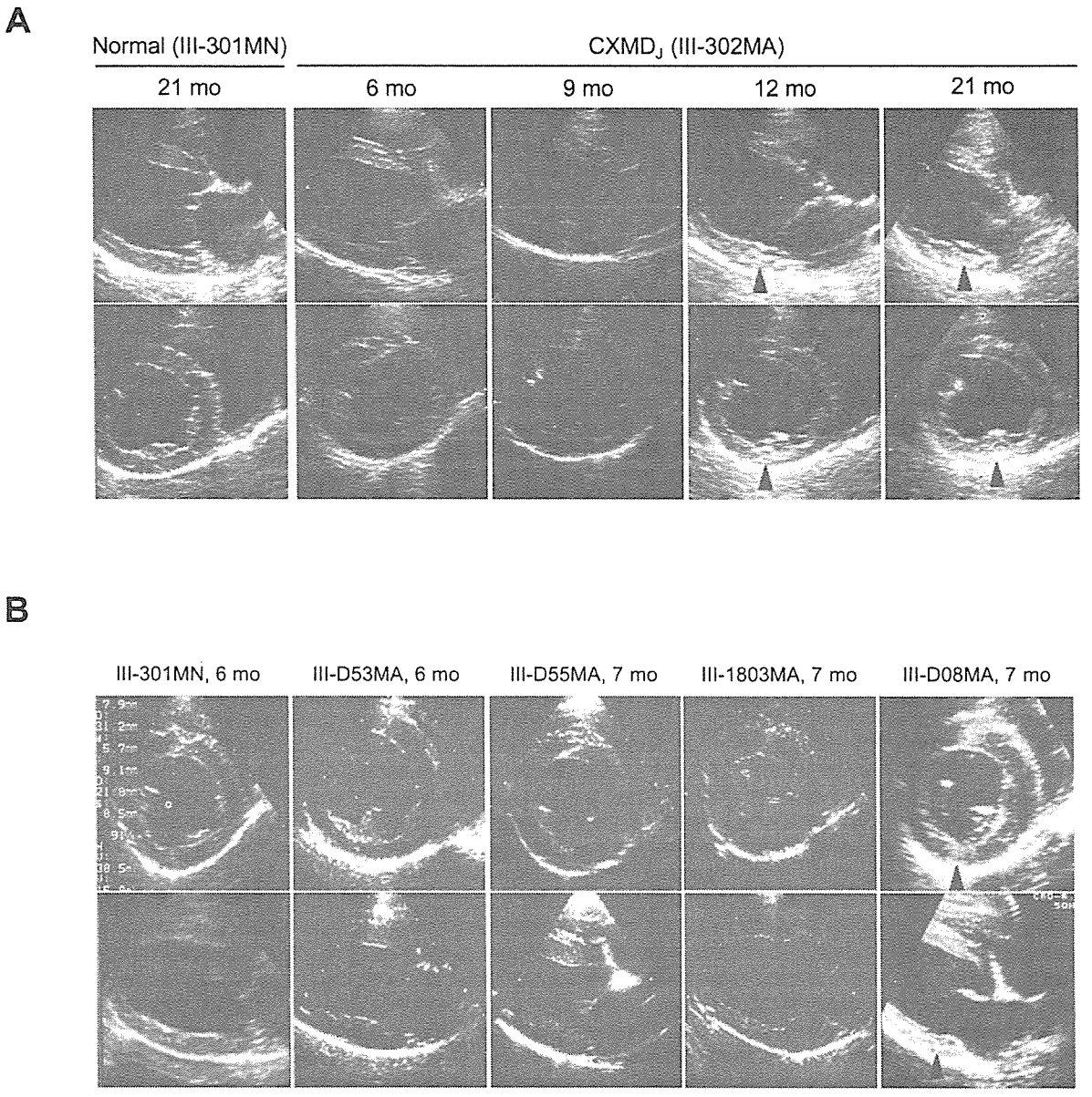

Figure 4
Echogenicity in CXMD$_J$ A: Sequential studies in echogenicity with advancing age by two-dimensional echocardiography in a normal dog III-301MN, and a CXMD$_J$ dog III-302MA, at 6–21 months of age. Hyperechoic lesions (arrowheads) of the left ventricular posterior wall were detected in the CXMD$_J$ dog at 12 months of age and older.**B**: Two-dimensional echocardiograms of a normal dog III-301MN at 6 months of age, and four CXMD$_J$ dogs III-D53MA, III-D55MA, III-1803MA, and III-D08MA at 6 to 7 months of age. The hyperechoic lesion (arrowhead) was detected only in the left ventricular posterior wall of III-D08MA.

Previous studies of morphology in GRMD showed that myocardial involvement is initially found in the left posterobasal ventricular wall, similar to that of patients with DMD [21-23]. Valentine *et al.* reported that GRMD dogs

Table 3: Echogenicity of left ventricular posterior wall in normal and CXMD$_J$ male dogs

	Months of age (mo)																			
	2	3	4	5	6	7	8	9	10	11	12	13	14	15	16	17	18	19	20	21
Normal dogs																				
III-D56MN					(-)*															
III-1804MN					(-)	(-)*														
III-D03MN	(-)			(-)		(-)			(-)			(-)	(-)*							
III-301 MN	(-)	(-)	(-)		(-)			(-)			(-)			(-)			(-)			(-)*
CXMD$_J$ dogs																				
III-D53MA					(-)*															
III-D55MA						(-)		*												
III-1803MA					(-)	(-)*														
III-D38MA											(-)*									
III-D02MA	(-)			(-)		(-)					(-)	(-)		(-)*						
III-D08MA	(-)			(+)		(+)					(+)	(+)		(+)*						
III-302MA	(-)	(-)	(-)		(-)			(-)			(+)			(+)			(+)			(+)*
III-303MA	(-)	(-)	(-)		(-)			(-)			(+)			(+)			(+)			(+)*

Hyperechoic lesion +, positive; -, negative; Asterisk in each CXMD$_J$ dog shows age at euthanasia.

at 6.5 months of age had acute severe lesions with focal myocardial mineralization associated macrophages and giant cells in the left ventricular papillary muscle and left ventricular wall [22]. Moreover, GRMD dogs at 12 months of age or older demonstrated prominent myocardial fibrosis in more widespread lesions [22]. The myocardial fibrosis of the left ventricular wall in the older stage of CXMD$_J$ dogs was consistent with that in DMD patients and GRMD dogs. The change was detected at 15 months of age or older in the CXMD$_J$ (III-D08MA, III-302MA, and III-303MA), although III-D08MA showed a hyperechoic lesion at 5 months of age or older (Table 3). The cardiac involvement in CXMD$_J$, therefore, was milder and slowly progressed than that in GRMD, although a longer period evaluation of large numbers of CXMD$_J$ will be needed to conclude the mild cardiac phenotypes of CXMD$_J$.

Why is the cardiac involvement in CXMD$_J$ milder than that in GRMD? Valentine *et al.* reported that skeletal muscle involvement in small dystrophic dogs was milder than that in large ones [19]. Several reports on dystrophic features have hypothesized that the clinical severity may be associated with growth rate [34] or muscle fiber diameter [35]. Living in a cage rather than running free could also affect the cardiac phenotypes of CXMD$_J$ because physical exercise promotes cardiac involvement in dystrophin-deficient *mdx* mice [36]. The difference in the genetic background between GRMD, golden retriever and CXMD$_J$, Beagle might also affect the disease progression.

The prominent deep Q-waves seen in both DMD and GRMD have been attributed to a reduction in or a loss of electromotive force caused by scarring of the posterobasal region of the left ventricle [8,9,17]. In our study, the deep Q-waves and increases in the Q/R ratio in CXMD$_J$ preceded the lesions seen on echocardiogram and histopathology, as shown in Fig. 6. Considering this result, the origin of the distinctive Q-waves might not be associated with the myocardial lesion in the posterobasal left ventricular wall. It has recently been reported that expression of a transgene in *mdx* mice for neuronal nitric oxide synthase (nNOS), which occurs as a secondary loss in dystrophin deficiency, decreased cardiac inflammation and fibrosis resulting in amelioration of both cardiac function and electrocardiographic abnormalities, including deep Q-waves [37]. Perloff *et al.* suggested that the alteration of a particular ionic current by lack of specific membrane proteins associated with dystrophin might participate in electrocardiographic changes [17]. We will not therefore deny that minimal myocardial damage could be associated with the pathogenesis of deep Q-waves, but our results suggest that an investigation of the conduction and cardiovascular systems will also be needed to explore the pathophysiology of the deep Q-waves in dystrophin-deficient heart. In this regard, CXMD$_J$ will be very useful to elucidate aspects of the dystrophin-deficient heart, but we may recognize that a longer period of time would be required to complete cardiac phenotypes in CXMD$_J$.

Conclusion

We demonstrated that the cardiac phenotypes of CXMD$_J$ are comparable to but milder than those of GRMD. Furthermore, we found for the first time that the distinct deep Q-waves precede detection of the left ventricular posterobasal lesion by echocardiography or histopathology. CXMD$_J$ may provide not only new insights into the mech-